RSC Advances

PAPER

View Article Online
View Journal | View Issue

Cite this: *RSC Adv.*, 2023, **13**, 16078

Research on the catalytic activity of MNP-[Dop-OH]-$CuBr_2$ nanocomposites: novel and stable reusable nanocatalysts for the synthesis of 1,3,5-triazine derivatives†

Shouchun Feng,*[a] Jinwang Tan,[a] Yufan Ma[a] and Li-Yuan Chang *[b]

In recent years, magnetic nanocatalysts have been recommended as one of the best catalysts by chemists. Among magnetic nanoparticles, Fe_3O_4 nanoparticles are highly suitable due to their magnetic properties, chemical stability and low toxicity. These catalysts can be separated *via* magnetic separation after the chemical process is over and reused after regeneration. Owing to the importance of 1,3,5-triazine derivatives in pharmaceutical and medicinal chemistry, the synthesis of these compounds is always one of the important goals of organic chemists. In this research work, we first successfully synthesized $CuBr_2$ immobilized on magnetic Fe_3O_4 nanoparticles functionalized with Dop-OH (prepared *via* the reaction of MNP-dopamine with 2-phenyloxirane) nanocomposites and then investigated their catalytic application in the synthesis of 1,3,5-triazine derivatives *via* an oxidative coupling reaction of amidine hydrochlorides and alcohols in air. Recycling experiments clearly revealed that MNP-[Dop-OH]-$CuBr_2$ nanocatalysts could be reused for at least 8 times without much loss of catalytic activity.

Received 5th April 2023
Accepted 12th May 2023

DOI: 10.1039/d3ra02261g

rsc.li/rsc-advances

Introduction

Due to the importance and various applications of catalysts in the fields of oil, automobile, pharmaceutical and food industries, they significantly relate fundamental and applied sciences to new technologies.[1–3] The modern science of chemistry, especially in the field of catalysis, involves the use of nanoparticles and nanomaterials in chemical reactions.[4] With the introduction of nano technology into the industry of catalysts, nanocatalysts have gained much interest. In most cases, these catalysts have shown remarkable properties and entered industrial processes.[5] Despite the high use of nanocatalysts, it is not easy to separate these nanocatalysts from the reaction mixture, and conventional separation methods such as filtering are not effective due to the nano size of these catalysts.[6–8] These limitations hinder the use of these nanocatalysts economically.[8] To overcome this problem, the use of magnetic nanoparticles seems to be a suitable solution.[9] In recent years, magnetic nanocatalysts have been recommended as one of the best catalysts by chemists. Magnetic nanoparticles are very suitable supports for linking catalysts.[10] These catalysts can be separated *via* magnetic separation after the chemical process is over and reused after regeneration.[11] Among magnetic nanoparticles, Fe_3O_4 nanoparticles are highly suitable due to their magnetic properties, chemical stability, and low toxicity.[12] During the last decade, the immobilization of metallic catalysts such as copper, palladium, nickel and zinc on the surface of Fe_3O_4 nanoparticles modified with ligands has been widely utilized as an efficient and attractive catalytic strategy for the performance of chemical reactions.[13–15]

Owing to the importance of heterocyclic compounds in medicinal chemistry and the synthesis of pharmaceutical and chemical compounds, the synthesis of these compounds is always one of the important goals of organic chemists.[16–18] Triazine cores are a very important part of antimicrobial, analgesic and anti-inflammatory drugs. 1,3,5-Triazines are a group of antibacterial and antifungal compounds that have a wide range of activities due to their low toxicity and high effectiveness.[19] A number of bioactive molecules and drugs with 1,3,5-triazine cores are displayed in Fig. 1.[20–22] Substituted 1,3,5-triazines are usually synthesized in two different ways. The classic method is based on the nucleophilic substitution of chlorine atoms in the starting material 2,4,6-trichloro-1,3,5-triazine, *i.e.*, cyanuric chloride. Another approach to synthesis is the sequential construction of a triazine ring. The best synthetic methods for the generation of 1,3,5-triazine are the transition metal-catalyzed condensation of 1,1-dibromoalkenes or alcohols and biguanides under mild conditions.[23] Considering the wide range of medicinal and biological applications of 1,3,5-triazine derivatives, various catalytic methods for the

[a]*Department of Chemical Engineering Tianjin Renai Coll, Tianjin 301636, PR China. E-mail: fengsc@tjrac.edu.cn*

[b]*Chemical Nanotechnology Research Institute, Shanghai, China. E-mail: liyuanchang839@gmail.com*

† Electronic supplementary information (ESI) available. See DOI: https://doi.org/10.1039/d3ra02261g

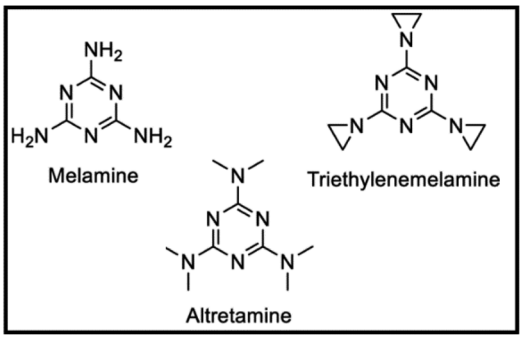

Fig. 1 Several examples of bioactive molecules with 1,3,5-triazine cores.

synthesis of these compounds were reported in the literature, but most of these methods used harsh conditions including toxic solvents and catalytic species, required high temperatures and generated low yields. In this regard, research on new and efficient methods for the synthesis of these compounds is an important priority among chemists.

In this research work, we first successfully synthesized $CuBr_2$ immobilized on magnetic Fe_3O_4 nanoparticles functionalized with Dop-OH (prepared *via* the reaction of MNP-dopamine with 2-phenyloxirane) nanocomposites and then investigated its catalytic application in the synthesis of 1,3,5-triazine derivatives *via* an oxidative coupling reaction of amidine hydrochlorides and alcohols in air.

Result and discussion

A general schematic of the preparation steps of MNP-[Dop-OH]-$CuBr_2$ nanocatalysts is shown in Scheme 1. First, magnetic iron nanoparticles and MNP-dopamine nanocomposites were synthesized by previously reported methods. In the next step, MNP-dopamine nanocomposites were reacted with 2-phenyloxirane in nitro methane for 6 h, followed by the embolization of copper(II) acetate for the preparation of the final nanocatalyst [MNP-[Dop-OH]-$CuBr_2$]. The structure of MNP-[Dop-OH]-$CuBr_2$ nanocatalysts was well characterized by a series of analyses such as FT-IR spectroscopy, SEM, TEM, EDX spectroscopy, MAP, TGA, VSM, XRD and ICP-OES.

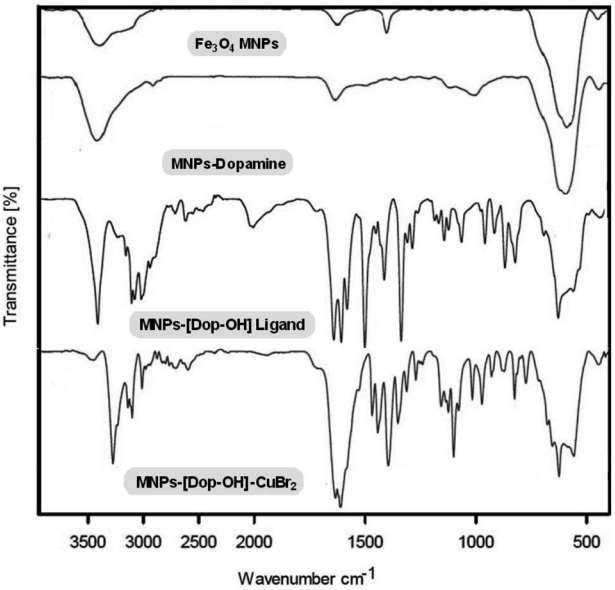

Fig. 2 FT-IR analysis of the preparation steps of MNP-[Dop-OH]-$CuBr_2$ nanocatalysts.

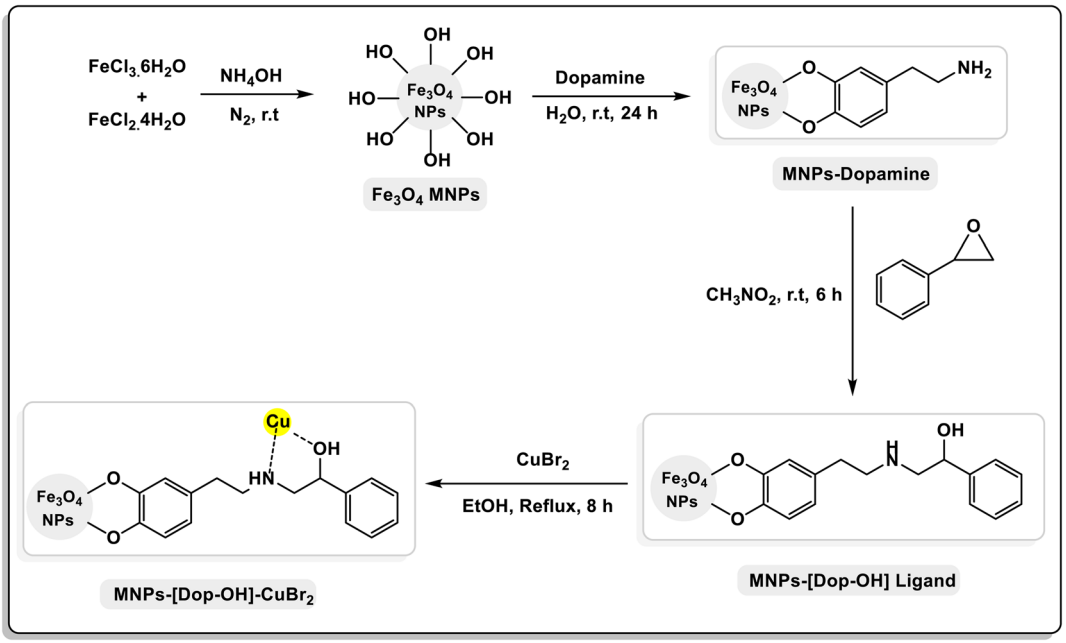

Scheme 1 General schematic of the preparation steps of MNP-[Dop-OH]-$CuBr_2$ nanocatalysts.

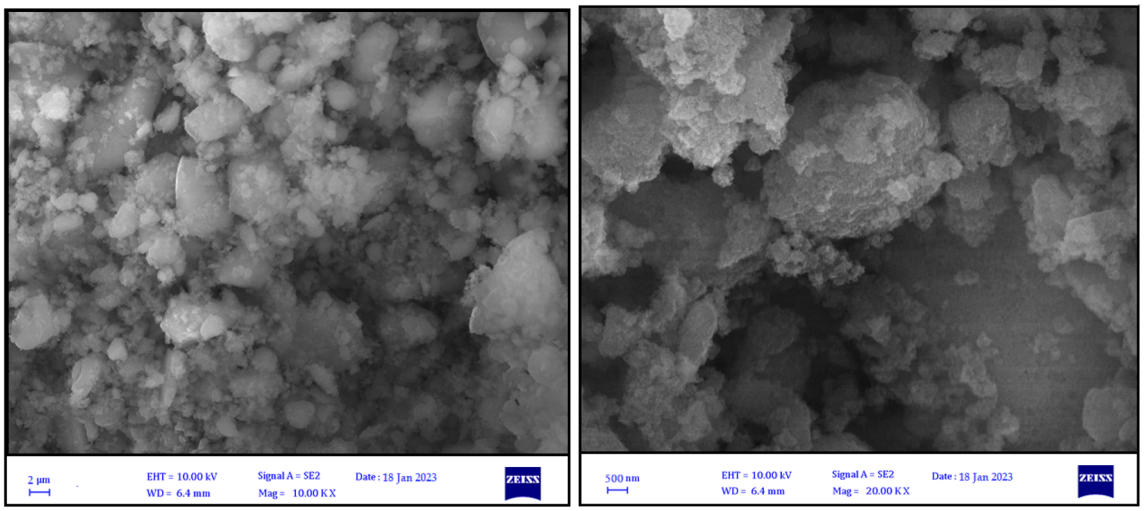

Fig. 3 SEM images of MNP-[Dop-OH]-$CuBr_2$ nanocatalysts at different magnifications.

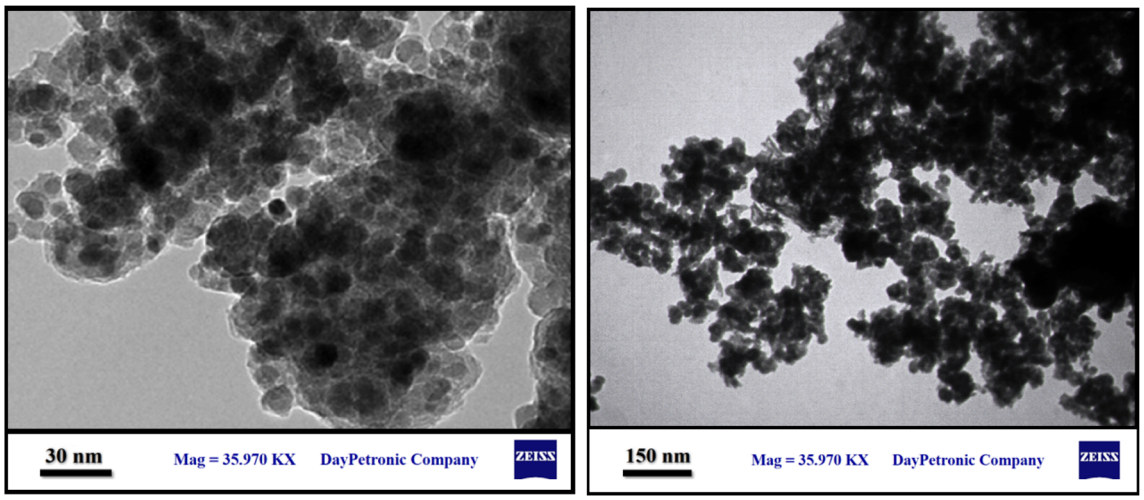

Fig. 4 TEM images of MNP-[Dop-OH]-$CuBr_2$ nanocatalysts at different magnifications.

FT-IR technique was used to detect the functional groups fixed on nanoparticles. An obvious peak in the region of 574 cm^{-1} indicates the presence of Fe–O bonding, and the broad absorption peak in the region of 3350 cm^{-1} is also attributed to the O–H stretching vibrations. In the spectrum of MNP-dopamine and MNP-[Dop-OH] ligand, C–H stretching vibrations appeared near 2700 cm^{-1}; and the peak that appeared in the region of 3400 cm^{-1} is related to the N–H group, which overlaps with the O–H stretching vibrations. Moreover, the peaks in the regions of 1200–1500 cm^{-1} confirm the formation of C–N and C–O bonds in the non-catalyst structure. In the infrared spectrum of MNP-[Dop-OH]-$CuBr_2$ nanocatalysts, it shows a peak in the region of 1623 cm^{-1} assigned to the C–N stretching vibration of the copper complex (Fig. 2).[15]

SEM and TEM techniques were used to identify MNP-[Dop-OH]-$CuBr_2$ nanocatalysts, which show the nanocatalyst surface at a very high magnification (Fig. 3 and 4). The SEM images show that the nano-catalyst particles have been synthesized on a scale of less than 25 nm. Moreover, this image shows that the nano catalyst particles were synthesized in uniform and equal sizes and their shape was spherical.

Energy-dispersive X-ray analysis (EDX) was applied to study the elements existing in the structure of the as-fabricated MNP-[Dop-OH]-$CuBr_2$ nanocatalyst. The presence of Fe, C, O, N and Cu peaks confirmed the construction of MNP-[Dop-OH]-$CuBr_2$ nanocatalysts (Fig. 5).

X-ray diffraction analysis was used to identify the crystal structure of Fe_3O_4 MNPs and MNP-[Dop-OH]-$CuBr_2$ nanocatalysts. As shown in Fig. 6, the target nanocatalyst was synthesized without changing the crystal structure of the Fe_3O_4 core, and the peaks observed in the X-ray diffraction pattern confirmed this issue. The diffraction pattern includes peaks (220), (311), (400), (422), (511) and (440), which indicates that the structure of the magnetic Fe_3O_4 nanoparticle was not destroyed during functionalization .[12]

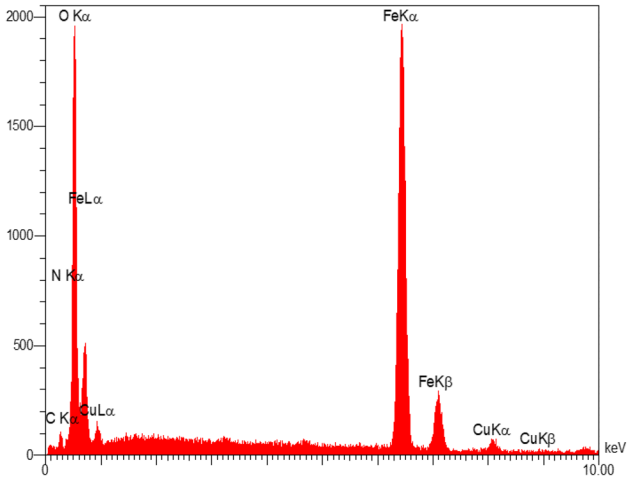

Fig. 5 EDX analysis of MNP-[Dop-OH]-$CuBr_2$ nanocatalysts.

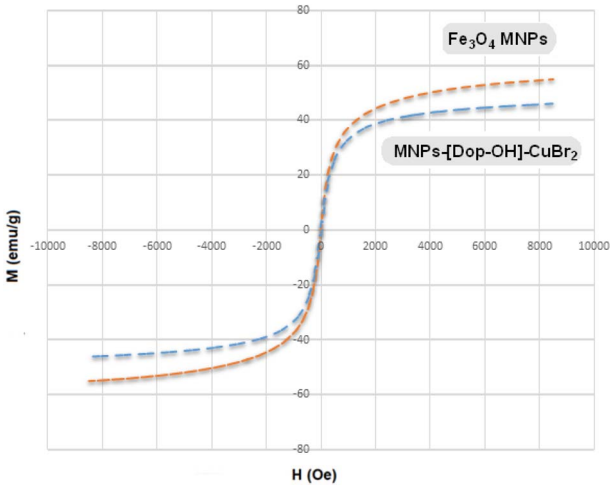

Fig. 7 VSM analysis of Fe_3O_4 MNPs and MNP-[Dop-OH]-$CuBr_2$ nanocatalysts.

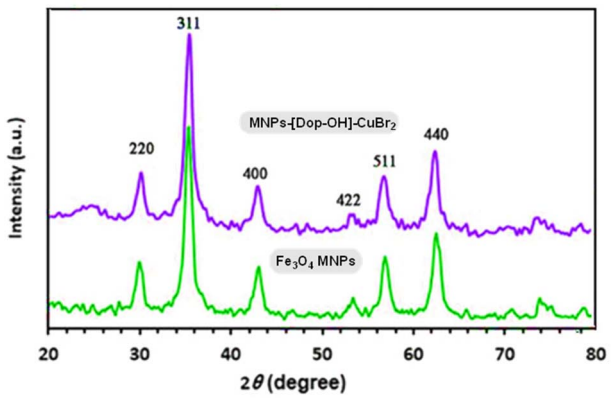

Fig. 6 XRD analysis of Fe_3O_4 MNPs and MNP-[Dop-OH]-$CuBr_2$ nanocatalysts.

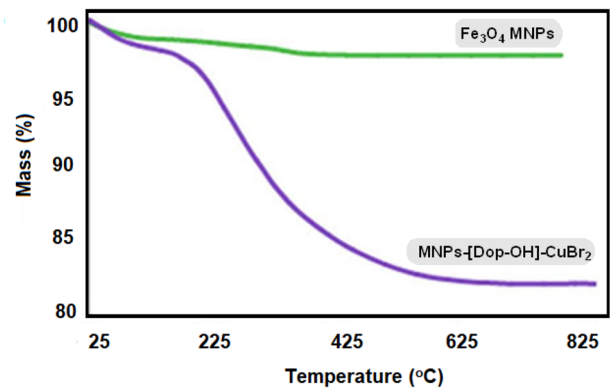

Fig. 8 TGA analysis of Fe_3O_4 MNPs and MNP-[Dop-OH]-$CuBr_2$ nanocatalysts.

Vibrating-sample magnetometry (VSM) analysis was used to check the magnetic properties of the synthesized MNP-[Dop-OH]-$CuBr_2$ nanocatalyst. As shown in Fig. 7, the magnetic property of MNP-[Dop-OH]-$CuBr_2$ shows a slight decrease compared to the magnetic property of iron nanoparticles, which indicates the stabilization of organic groups and copper complex on the surface of nanoparticles.

Thermogravimetric analysis (TGA) was used to detect the percentage of organic groups fixed on the surface of magnetic iron nanoparticles. As shown in Fig. 8, the weight loss observed at temperatures below 200 °C is related to surface absorbed water and other solvents. The complete decomposition of organic groups placed on magnetic iron nanoparticles is observed in the temperature range of 250–550 °C, which is approximately 20%. This confirms the fact that this nanocatalyst can easily be used in organic reactions with and a high temperature range should be used. The ICP-OES technique was used to determine the amount of Cu coordinated on the functionalized iron nanoparticles, and it was found that the amount of copper stabilized on the nanoparticles is 14.23×10^{-5} mol g^{-1}.

At the beginning of the laboratory works for the synthesis of 1,3,5-triazine derivatives, to obtain the optimal reaction conditions, the oxidative coupling reaction of benzamidine hydrochloride with benzyl alcohol (product **3a**) was selected as the model reaction, and the effects of different parameters including temperature, solvent, base and amount of catalyst were investigated on this reaction. The results of these experiments are listed in Table 1. To investigate the effect of the amount of catalyst on the progress of the reaction, the model reaction was carried out in the absence of the catalyst, and the reaction failed under these conditions. By increasing the amount of the catalyst, the reaction progressed significantly, but the amounts above 20 mg did not have much effect on the reaction progress. Therefore, the amount of 20 mg was chosen as the optimal amount for the reaction. A trace amount of the model products were seen in the absence of bases. Amongst tested bases, the best results were shown in the presence of

Table 1 Optimization of reaction conditions for the reaction of benzamidine hydrochloride with benzyl alcohol (product 3a)

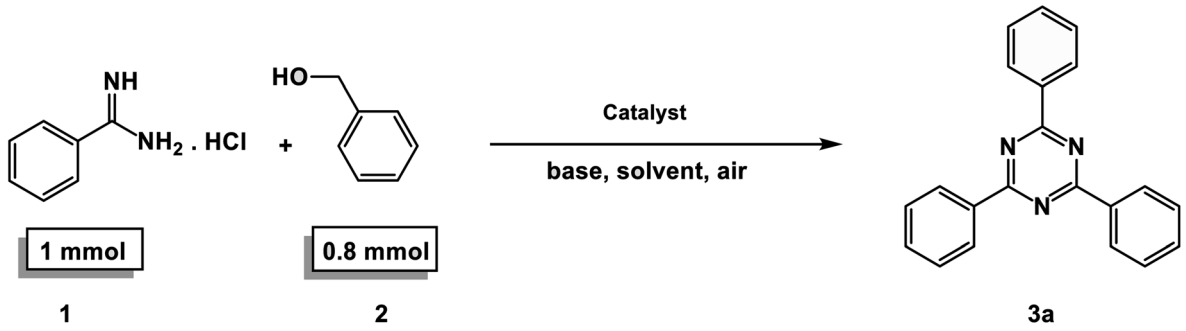

Entry	Catalyst (mg)	Base	Solvent (tem. °C)	Time (h)	Yield[a] (%)	TON	TOF (h^{-1})
1	—	K_2CO_3	DMF (reflux)	24	—	—	—
2	MNPs-[Dop-OH]-$CuBr_2$ (5)	K_2CO_3	DMF (reflux)	14	39	5414	386.7
3	MNPs-[Dop-OH]-$CuBr_2$ (10)	K_2CO_3	DMF (reflux)	12	73	5069	422.45
4	MNPs-[Dop-OH]-$CuBr_2$ (15)	K_2CO_3	DMF (reflux)	9	85	3990	399
5	MNPs-[Dop-OH]-$CuBr_2$ (20)	K_2CO_3	DMF (reflux)	9	90	3169	352.1
6	MNPs-[Dop-OH]-$CuBr_2$ (25)	K_2CO_3	DMF (reflux)	9	90	2500	277
7	MNPs-[Dop-OH]-$CuBr_2$ (20)	—	DMF (reflux)	24	Trace	0	0
8	MNPs-[Dop-OH]-$CuBr_2$ (20)	KOH	DMF (reflux)	9	42	1458	162
9	MNPs-[Dop-OH]-$CuBr_2$ (20)	KOAc	DMF (reflux)	9	94	3263	362.6
10	MNPs-[Dop-OH]-$CuBr_2$ (20)	Cs_2CO_3	DMF (reflux)	9	86	2986	331.7
11	MNPs-[Dop-OH]-$CuBr_2$ (20)	KF	DMF (reflux)	9	53	1840	204.4
12	MNPs-[Dop-OH]-$CuBr_2$ (20)	NaOH	DMF (reflux)	9	29	1006	111.8
13	MNPs-[Dop-OH]-$CuBr_2$ (20)	Na_2CO_3	DMF (reflux)	9	85	2951	327.9
14	MNPs-[Dop-OH]-$CuBr_2$ (20)	*t*-BuOK	DMF (reflux)	9	11	381	42.4
15	MNPs-[Dop-OH]-$CuBr_2$ (20)	NaHCO3	DMF (reflux)	9	59	2048	227.6
16	MNPs-[Dop-OH]-$CuBr_2$ (20)	KOAc	Water (reflux)	9	68	2361	262.3
17	MNPs-[Dop-OH]-$CuBr_2$ (20)	KOAc	DMSO (reflux)	9	75	2604	289.3
18	MNPs-[Dop-OH]-$CuBr_2$ (20)	KOAc	PEG (100 °C)	9	95	3298	366.5
19	MNPs-[Dop-OH]-$CuBr_2$ (20)	KOAc	THF (reflux)	9	69	2395	266.2
20	MNPs-[Dop-OH]-$CuBr_2$ (20)	KOAc	Toluene (reflux)	9	89	3090	343.3
21	MNPs-[Dop-OH]-$CuBr_2$ (20)	KOAc	EtOH (reflux)	9	53	1840	204.4
22	MNPs-[Dop-OH]-$CuBr_2$ (20)	KOAc	Solvent-free (100 °C)	12	6	208	17.3
23	MNPs-[Dop-OH]-$CuBr_2$ (20)	KOAc	PEG (90 °C)	9	89	3090	343.3
24	MNPs-[Dop-OH]-$CuBr_2$ (20)	KOAc	PEG (110 °C)	9	96	3333	370.3
25	**MNPs-[Dop-OH]-$CuBr_2$ (20)**	**KOAc**	**PEG (120 °C)**	**8**	**98**	**3402**	**425.3**
26	MNPs-[Dop-OH]-$CuBr_2$ (20)	KOAc	PEG (130 °C)	8	98	3402	425.3
27	MNPs-[Dop-OH]-$CuBr_2$ (20)	KOAc	PEG (140 °C)	8	96	3333	416.6
28	—	KOAc	PEG (120 °C)	8	Trace	0	0
29	Fe_3O_4 MNPs (20)	KOAc	PEG (120 °C)	8	27	937	177.1
30	$CuBr_2$	KOAc	PEG (120 °C)	8	34	1180	147.5

[a] Isolated yield.

KOAc as the base. To find the medium reaction, the model reaction was tested in different solvents. The maximum yield and suitable time were observed in PEG at 120 °C after 8 h. To expand the scope of application of this synthetic method, the oxidative coupling reaction of different amidine hydrochlorides with a wide range of alcohols was studied under the standardized conditions (Table 2). Under this catalytic system, a wide range of aromatic alcohols with both electron-donating and electron-withdrawing substituents were successfully reacted with amidine hydrochlorides and the target products were synthesized in good to excellent yields. It is noteworthy that several functional groups, such as methyl, ethyl, isopropyl, methoxy, chloro, bromo, fluoro and nitro were well tolerated. All products are known and the physical properties of the corresponding products are in good agreement with the reported samples .[20–24]

Based on the literature search,[24] we present a tentative mechanism for the synthesis of 1,3,5-triazine derivatives *via* the oxidative coupling reaction of amidine hydrochlorides and alcohols catalyzed by MNP-[Dop-OH]-$CuBr_2$ nanocomposites under air conditions in Scheme 2.

The ability to recycle and reuse the catalyst is one of the most important features of heterogeneous catalytic systems, which makes these catalysts suitable for industrial

Table 2 Scope of the oxidative coupling reaction of amidine hydrochlorides and alcohols catalyzed by MNP-[Dop-OH]-$CuBr_2$ nanocomposites under air conditions[a]

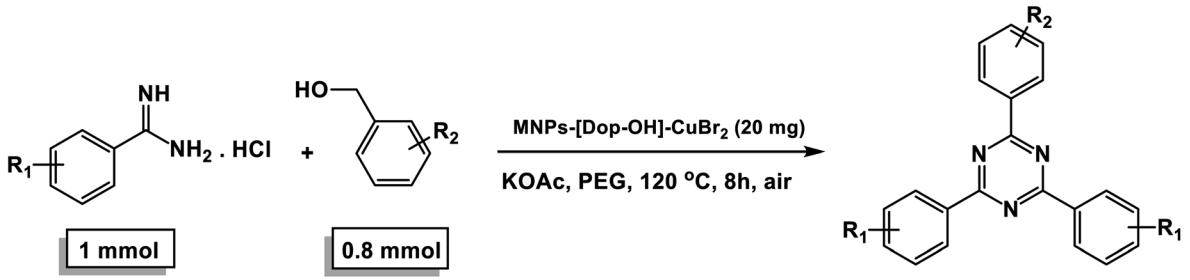

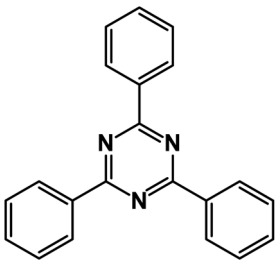

3a (98%)

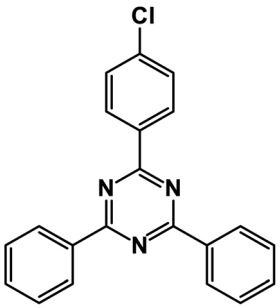

3b (99%)

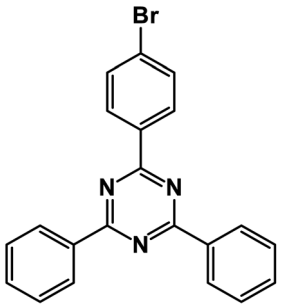

3c (99%)

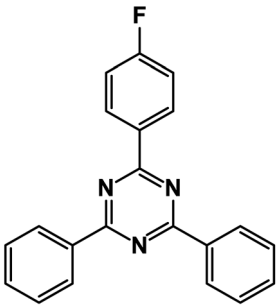

3d (96%)

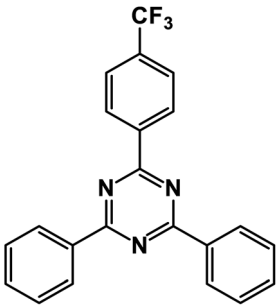

3e (93%)

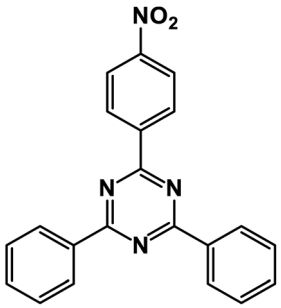

3f (97%)

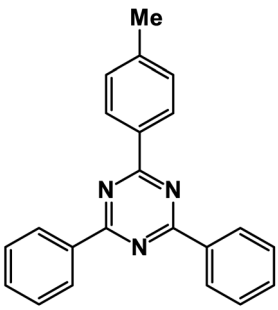

3g (94%)

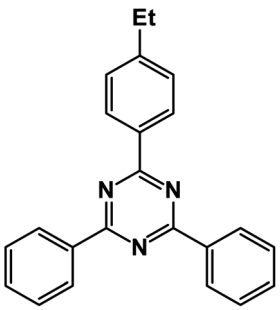

3h (92%)

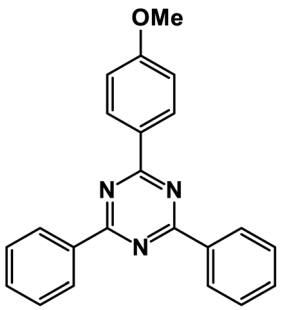

3i (93%)

Table 2 (*Contd.*)

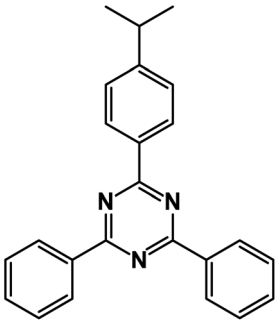

3j (90%)

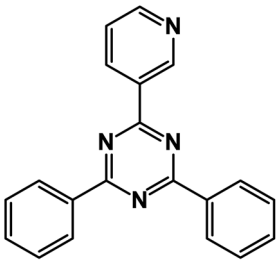

3k (92%)

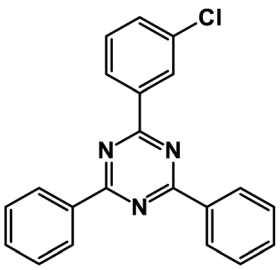

3l (92%)

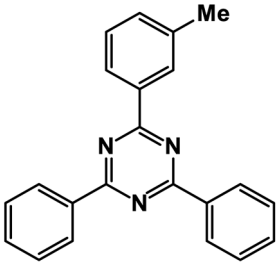

3m (88%)

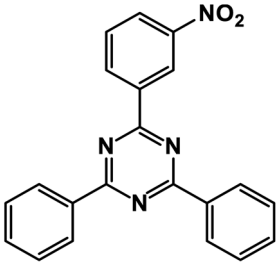

3n (91%)

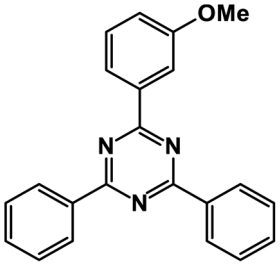

3o (89%)

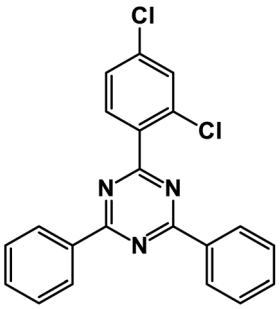

3p (94%)

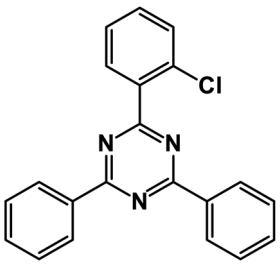

3q (93%)

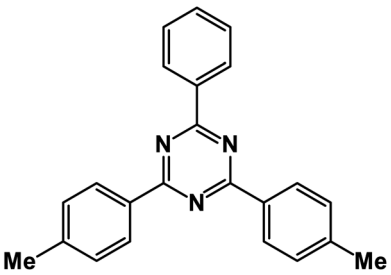

3r (94%)

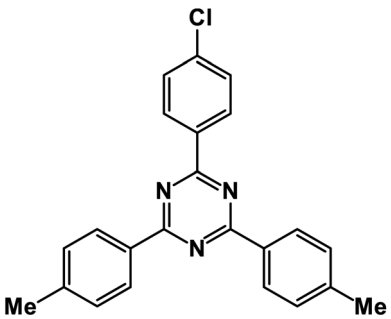

3s (92%)

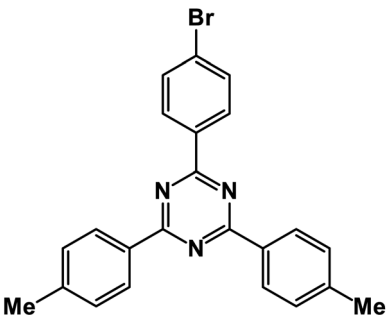

3t (93%)

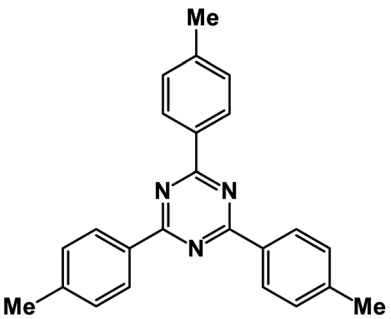

3u (90%)

[a] Isolated yield.

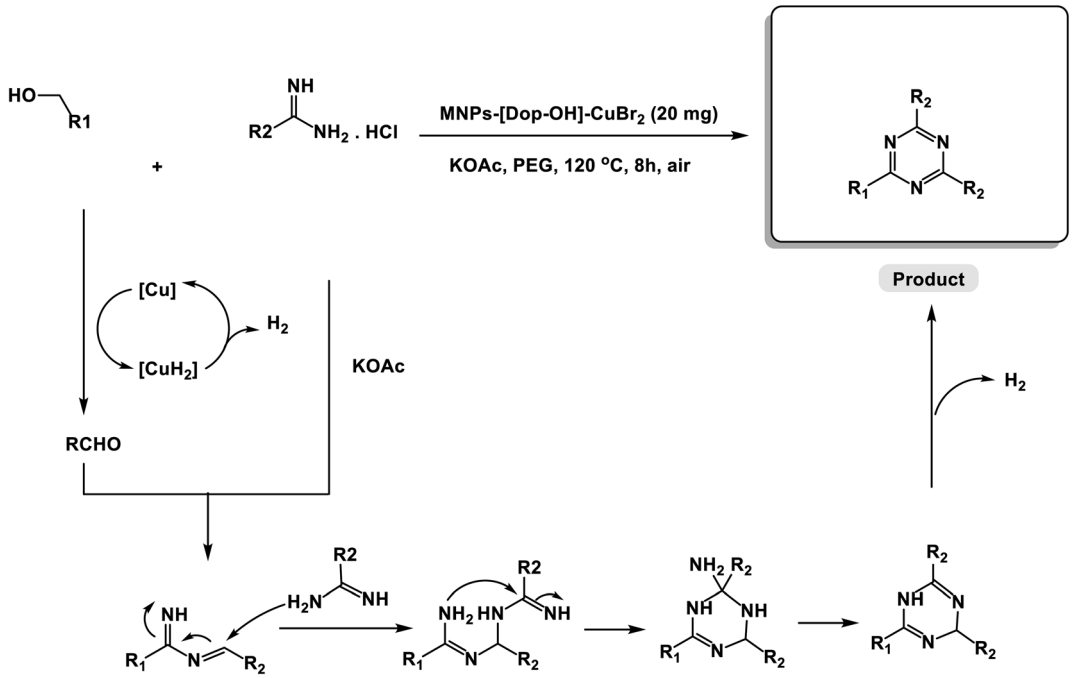

Scheme 2 Suggested mechanism for the oxidative coupling reaction of amidine hydrochlorides and alcohols catalyzed by MNP-[Dop-OH]-$CuBr_2$ nanocomposites under air conditions.

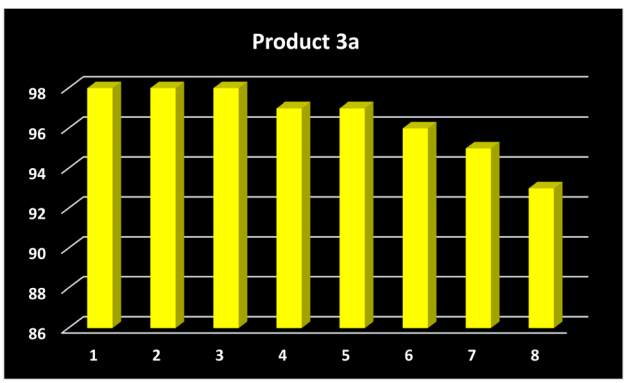

Fig. 9 Reusability of MNP-[Dop-OH]-$CuBr_2$ nanocatalysts in the preparation of product **3a**.

applications. In this respect, the reachability of the MNP-[Dop-OH]-$CuBr_2$ nanocatalyst was studied in the synthesis of model product **3a**. At the end of the reaction, the separated catalyst was washed with water and acetone using an external magnet. As shown in Fig. 9, the MNP-[Dop-OH]-$CuBr_2$ catalyst can be recycled and reused for 8 runs without any significant reduction in its catalytic activity. The ICP-OES analysis of the recovered MNP-[Dop-OH]-$CuBr_2$ catalyst (after 8 times) showed that the amount of copper stabilized on the nanoparticles is 14.12×10^{-5} mol g^{-1}. Moreover, XRD and VSM techniques revealed that the structure and magnetic property of the recovered MNP-[Dop-OH]-$CuBr_2$ catalyst was not changed after 8 times (Fig. 10 and 11).

As can be seen in Table 3, in order to evaluate how well MNP-[Dop-OH]-$CuBr_2$ functions as a catalyst for the oxidative coupling reaction of amidine hydrochlorides and alcohols, the acquired findings were compared to those that had been previously published for other catalytic systems in the scientific literature. This was done so that the performance of MNP-[Dop-OH]-$CuBr_2$ could be evaluated. This has recently suggested that the catalyst boasts a number of desirable qualities including rapid reaction durations, the capability to be recovered, a high reaction yield, the capability to be recycled through the use of a straightforward filtration method, the availability of starting materials that are both cheap and abundant, and non-toxicity.

Conclusion

In this work, we have successfully fabricated $CuBr_2$ immobilized on magnetic Fe_3O_4 nanoparticles functionalized with Dop-OH (prepared *via* the reaction of MNP-dopamine with 2-phenyloxirane) nanocomposites and well characterized its structure by a series of analyses such as FT-IR spectroscopy, SEM, TEM, EDX spectroscopy, MAP, TGA, VSM, XRD and ICP-OES. The catalytic behavior of the MNP-[Dop-OH]-$CuBr_2$ nanocatalyst was evaluated in the synthesis of 1,3,5-triazine derivatives *via* an oxidative coupling reaction of amidine hydrochlorides and alcohols in air. The experimental results clearly confirmed that the MNP-[Dop-OH]-$CuBr_2$ nanocomposite is a green, efficient and highly reusable catalyst in the synthesis of 1,3,5-triazine derivatives because both the target products were synthesized in high to excellent yields and that the MNP-[Dop-OH]-$CuBr_2$ nanocatalyst could be reused for at least 8 times without much loss of catalytic activity.

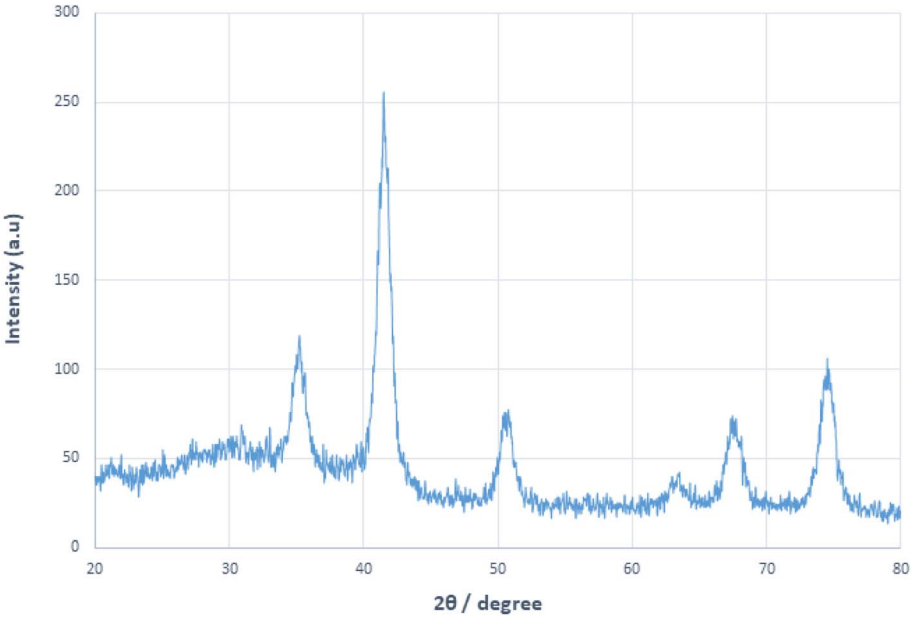

Fig. 10 XRD analysis of MNP-[Dop-OH]-$CuBr_2$ nanocatalysts after 8 runs.

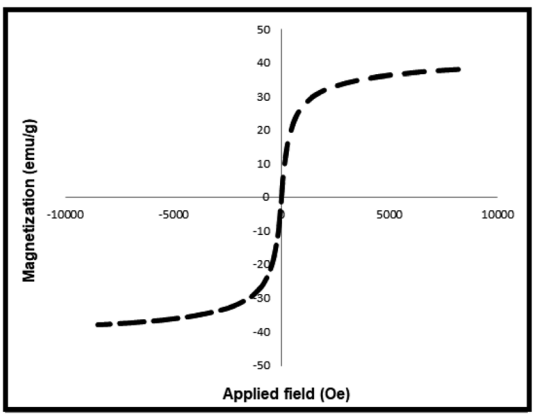

Fig. 11 VSM analysis of MNP-[Dop-OH]-$CuBr_2$ nanocatalysts after 8 runs.

Experimental

Chemicals were purchased from Fisher and Merck. The reagents and solvents used in this work were obtained from Sigma-Aldrich, Fluka or Merck and used without further purification. The infrared spectra (IR) of samples were recorded using a NICOLET impact 410 spectrometer with KBr disks. ^{1}HNMR and ^{13}CNMR spectra were recorded using a Bruker DRX-400 spectrometer at 400 and 100 MHz respectively.

General procedure for the preparation of 1,3,5-triazine derivatives catalyzed by MNP-[Dop-OH]-$CuBr_2$

A MNP-[Dop-OH]-$CuBr_2$ nanocomposite (20 mg) was added to a mixture of alcohols (0.8 mmol), benzamidine hydrochlorides (1.0 mmol), and K_2CO_3 (1.5 equiv.) in PEG (3 mL) in a flask, and the reaction was stirred at 120 °C under air conditions for 8 h. The progress of the reaction was monitored by thin layer chromatography (TLC). Then, the reaction was cooled down to room temperature followed by the separation of the catalyst using an external magnet. The resulting mixture was extracted several times with EtOAc (10 mL) and brine (5 mL). The organic phases were combined and dried with anhydrous Na_2SO_4 and evaporated under vacuum. The crude product was purified by column chromatography on the silica gel using petroleum ether/EtOAc (100 : 1) as an eluent to obtain 1,3,5-triazine products.

Table 3 Comparison of the catalytic activity of MNP-[Dop-OH]-$CuBr_2$ nanocatalysts with existing catalysts

Entry	Catalyst	Time (h)	Yield[a] (%)	Ref.
1	Potassium *tert*-butoxide	8	69	25
2	1,10-Phenanthroline, cupric acetate	24	89	26
3	*N*-Iodosuccinimide	16	88	27
4	Bis(dichloro(η6-*p*-cymene)ruthenium)	16	85	28
5	Nitrogen-doped carbon supported nanocobalt	16	51	29
6	$[Cp^*IrI_2]_2$/xantphos	20	85	30
7	MNPs-[Dop-OH]-$CuBr_2$ (20)	8	98	This work

[a] Isolated yields.

NMR data for 1,3,5-triazine products

*2,4,6-Triphenyl-1,3,5-triazine (product **3a**).*

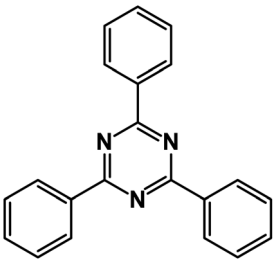

1H NMR (400.1 MHz, CDCl3): δ = 8.33–8.31 (d, J = 7.4 Hz, 4H), 7.91 (s, 2H), 7.87–7.85 (d, J = 7.4 Hz, 2H), 7.67–7.34 (m, 7H). 13C {1H} NMR (100.6 MHz, CDCl3): δ = 167.6, 139.8, 139.2, 129.3, 129.1, 129.1, 128.8, 127.3, 127.3.

*2-(4-Chlorophenyl)-4,6-diphenyl-1,3,5-triazine (product **3b**).*

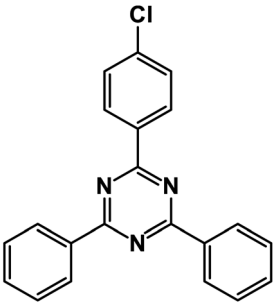

1H NMR (400.1 MHz, CDCl3): δ = 8.31–8.09 (d, J = 7.3 Hz, 4H), 7.92–7.85 (d, J = 8.5 Hz, 2H), 7.77–7.75 (s, 2H), 7.59–7.46 (m, 6H). 13C{1H} NMR (100.6 MHz, CDCl3): δ = 167.6, 166.2, 150.4, 139.4, 138.9, 138.0, 135.2, 129.2, 129.2, 129.1, 128.9, 128.8, 128.5, 127.2, 127.2, 117.4, 116.8.

*2-(4-Bromophenyl)-4,6-diphenyl-1,3,5-triazine (product **3c**).*

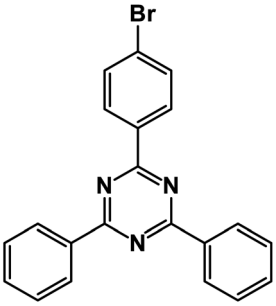

1H NMR (400.1 MHz, CDCl3): δ = 8.22 (d, J = 7.1 Hz, 2H), 8.18 (d, J = 8.6 Hz, 2H), 7.92 (s, 1H), 7.87 (s, 1H), 7.78–7.74 (d, J = 6.9 Hz, 2H), 7.66–7.64 (d, J = 8.6 Hz, 2H), 7.56–7.26 (m, 4H). 13C {1H} NMR (100.6 MHz, CDCl3): δ = 169.7, 167.3, 150.4, 140.5, 138.9, 139.5, 132.9, 130.3, 130.2, 130.2, 128.8, 128.8, 127.3, 126.2, 123.6, 118.5, 117.8.

*2-(4-Fluorophenyl)-4,6-diphenyl-1,3,5-triazine (product **3d**).*

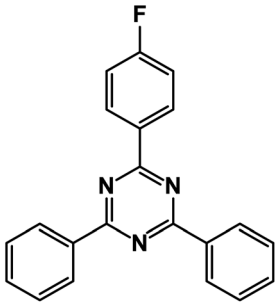

1H NMR (400.1 MHz, CDCl3): δ = 8.33–8.31 (d, J = 7.4 Hz, 2H), 7.89 (s, 2H), 7.58–7.28 (m, 9H), 7.20–7.16 (m, 1H). 13C{1H} NMR (100.6 MHz, CDCl3): δ = 165.7, 163.2, 157.8, 150.0, 142.5 (d, J = 7.8 Hz), 140.5, 131.8 (d, J = 8.3 Hz), 130.3, 129.9, 128.3, 126.4, 124.0 (d, J = 2.8 Hz), 118.0, 117.0 (d, J = 21.1 Hz), 116.9, 113.3 (d, J = 22.4 Hz).

*2,4-Diphenyl-6-(4-(trifluoromethyl)phenyl)-1,3,5-triazine (product **3e**).*

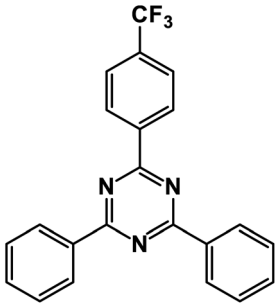

1H NMR (400.1 MHz, CDCl3): δ = 8.36 (d, J = 8.3 Hz, 2H), 8.23 (d, J = 7.0 Hz, 2H), 7.97 (s, 1H), 7.93 (s, 1H), 7.79–7.76 (m, 2H), 7.59–7.47 (m, 6H). 13C{1H} NMR (100.6 MHz, CDCl3): δ = 158.8, 156.9, 151.5, 143.0, 140.3, 139.8, 130.9 (q, J = 32.3), 129.4, 129.3, 129.3, 128.9, 127.5, 127.3, 127.2, 125.7 (q, J = 3.8 Hz), 124.4 (q, J = 272.0 Hz), 119.9, 118.4.

*2-(4-Nitrophenyl)-4,6-diphenyl-1,3,5-triazine (product **3f**).*

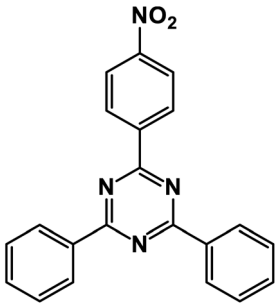

1H NMR (400.1 MHz, CDCl3): δ = 8.14 (d, J = 7.5 Hz, 2H), 7.70 (d, J = 7.5 Hz, 1H), 7.67 (s, 1H), 7.54–7.29 (m, 10H), 13C{1H} NMR (100.6 MHz, CDCl3): δ = 169.7, 163.8, 161.4, 141.8, 141.5, 139.3, 134.5, 130.1, 129.7, 129.6, 129.6, 129.6, 129.4, 128.1, 127.7, 125.0, 121.7.

*2,4-Diphenyl-6-(p-tolyl)-1,3,5-triazine (product **3g**).*

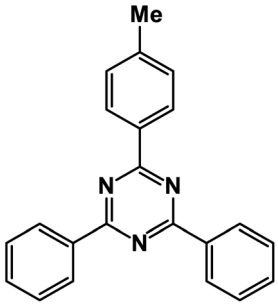

1H NMR (400.1 MHz, CDCl3): $\delta = 8.09$ (d, $J = 7.4$ Hz, 2H), 8.03 (d, $J = 7.4$ Hz, 2H), 7.63–7.53 (m, 4H), 7.51–7.43 (m, 5H), 7.41–7.40 (m, 2H), 13C{1H} NMR (100.6 MHz, CDCl3): δ = 166.2, 161.0, 153.9, 143.2, 139.2, 138.2, 134.2, 133.8, 129.5, 127.9, 127.8, 127.7, 127.4, 127.4126.0, 124.8, 23.1.

*2-(4-Ethylphenyl)-4,6-diphenyl-1,3,5-triazine (product **3h**).*

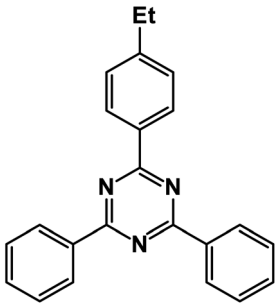

1H NMR (400.1 MHz, CDCl3): $\delta = 8.17$ (d, $J = 7.5$ Hz, 2H), 7.72 (d, $J = 7.5$ Hz, 1H), 7.63 (m, 3H), 7.55–7.41 (m, 8H), 13C{1H} NMR (100.6 MHz, CDCl3): $\delta = 170.7$, 164.8, 162.4, 141.8, 141.5, 139.3, 134.5, 130.1, 129.7, 129.6, 129.6, 129.6, 129.4, 128.1, 127.7, 124.0, 120.7, 22.4, 14.9.

*2-(4-Methoxyphenyl)-4,6-diphenyl-1,3,5-triazine (product **3i**).*

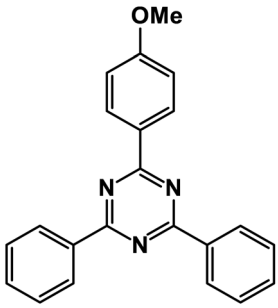

1H NMR (400.1 MHz, CDCl3): $\delta = 8.15$ (d, $J = 7.6$ Hz, 2H), 7.75–7.70 (m, 2H), 7.67 (s, 1H), 7.56–7.41 (m, 9H), 13C{1H} NMR (100.6 MHz, CDCl3): $\delta = 169.6$, 164.2, 161.7, 142.6, 141.4, 139.5, 130.6, 129.9, 129.7, 129.7, 129.6, 128.2, 128.0, 128.0, 128.1, 12.0, 121.1, 58.1.

*2-(4-Isopropylphenyl)-4,6-diphenyl-1,3,5-triazine (product **3j**).*

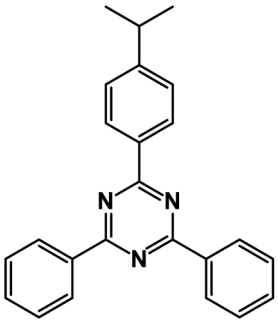

1H NMR (400.1 MHz, CDCl3): $\delta = 8.16$ (d, $J = 7.2$ Hz, 2H), 7.92 (s, 1H), 7.83 (s, 2H), 7.78 (d, $J = 7.0$ Hz, 2H), 7.58–7.47 (m, 7H), 13C{1H} NMR (100.6 MHz, CDCl3): δ = 166.8, 164.3, 160.1, 159.9, 144.3, 139.5, 137.9, 128.2, 128.2, 127.8, 126.3, 126.2, 118.0, 116.2, 33.2, 23.1.

*2,4-Diphenyl-6-(pyridin-3-yl)-1,3,5-triazine (product **3k**).*

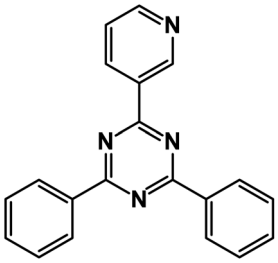

1H NMR (400.1 MHz, CDCl3): $\delta = 8.23$ (d, $J = 8.3$ Hz, 2H), 7.63 (s, 1H), 7.54–7.43 (m, 9H), 7.36 (t, $J = 7.4$ Hz, 1H), 7.23 (d, $J = 8.5$ Hz, 1H), 13C{1H} NMR (100.6 MHz, CDCl3): δ = 164.5, 162.3, 159.4, 139.7, 139.5, 137.3, 135.4, 128.2, 127.9, 127.8, 127.8, 127.6, 127.1, 127.0, 126.6, 125.2, 125.9, 123.9, 120.0.

*2-(3-Chlorophenyl)-4,6-diphenyl-1,3,5-triazine (product **3l**).*

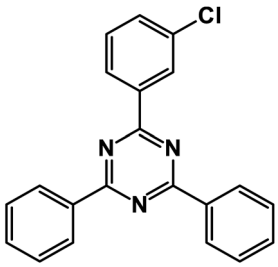

1H NMR (400.1 MHz, CDCl3): $\delta = 8.15$ (d, $J = 8.6$ Hz, 2H), 8.09 (d, $J = 8.6$ Hz, 2H), 7.88 (s, 2H), 7.76 (d, $J = 6.9$ Hz, 2H), 7.67 (d, $J = 8.6$ Hz, 2H), 7.63–7.47 (m, 4H). 13C{1H} NMR (100.6 MHz, CDCl3): $\delta = 156.6$, 156.5, 150.8, 138.8, 138.4, 137.9, 135.5, 132.0, 129.4, 129.3, 129.1, 128.8, 128.5, 127.3, 123.8, 117.3, 117.2.

*2-(3-Methylphenyl)-4,6-diphenyl-1,3,5-triazine (product **3m**).*

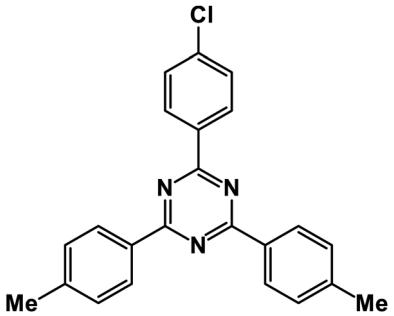

1H NMR (400.1 MHz, CDCl3): $\delta = 8.29$ (d, $J = 7.5$ Hz, 2H), 7.93 (s, 2H), 7.68 (d, $J = 7.7$ Hz, 2H), 7.58–7.53 (m, 4H), 7.48 (t, 2H), 7.38 (d, $J = 7.7$ Hz, 2H), 13C{1H} NMR (100.6 MHz, CDCl3): $\delta =$ 167.5, 160.1, 140.8, 140.1, 137.2, 129.9, 128.1, 127.8, 126.2, 126.1, 118.0, 22.3.

*2-(3-Nitrophenyl)-4,6-diphenyl-1,3,5-triazine (product **3n**).*

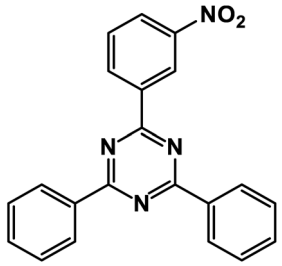

1H NMR (400.1 MHz, CDCl3): $\delta =$ 8.75–8.70 (t, 1H), 8.68 (s, 1H), 8.25 (d, $J = 7.3$ Hz, 2H), 8.02 (s, 1H), 7.89–7.84 (m, 3H), 7.58–7.51 (m, 4H), 7.49–7.46 (m, 2H), 13C{1H} NMR (100.6 MHz, CDCl3): $\delta =$ 167.3, 166.5, 166.4, 160.4, 140.2, 140.0, 138.9, 137.0, 128.2, 128.1, 128, 127.9, 127.4, 126.2, 124.9, 122.6, 118.6, 116.7.

*2-(3-Methoxyphenyl)-4,6-diphenyl-1,3,5-triazine (product **3o**).*

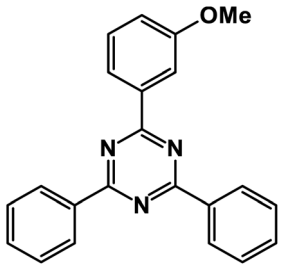

1H NMR (400.1 MHz, CDCl3): $\delta = 8.24$ (d, $J = 7.8$ Hz, 2H), 8.21 (d, $J = 8.8$ Hz, 2H), 7.86 (s, 1H), 7.85 (s, 1H), 7.78 (d, $J = 7.2$ Hz, 2H), 7.55–7.43 (m, 6H), 13C{1H} NMR (100.6 MHz, CDCl3): $\delta =$ 161.7, 158.5, 158.2, 151.2, 139.8, 138.3, 133.4, 129.2, 129.1, 129.0, 128.8, 128.5, 127.3, 127.2, 117.6, 117.4, 115.2, 56.5.

*2-(2,4-Dichlorophenyl)-4,6-diphenyl-1,3,5-triazine (product **3p**).*

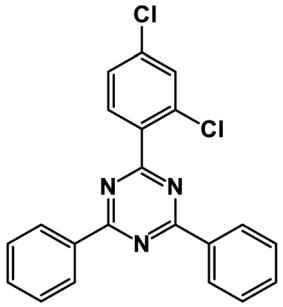

1H NMR (400.1 MHz, CDCl3): $\delta = 8.71$ (d, $J = 4.0$ Hz, 1H), 8.61–8.58 (m, 2H), 7.97 (t, 1H), 7.87–7.82 (m, 3H), 7.58 (s, 1H), 7.53–7.43 (m, 3H), 7.32 (dd, $J = 5.0$ Hz, $J = 6.5$ Hz, 1H), 7.26 (d, $J =$ 3.3 Hz, 1H), 13C{1H} NMR (100.6 MHz, CDCl3): $\delta =$ 156.4, 156.1, 154.3, 150.1, 149.4, 149.2, 143.3, 138.5, 136.8, 129.1, 129.0, 127.1, 123.9, 121.5, 117.3, 116.4, 112.2, 108.9.

*2-(2-Chlorophenyl)-4,6-diphenyl-1,3,5-triazine (product **3q**).*

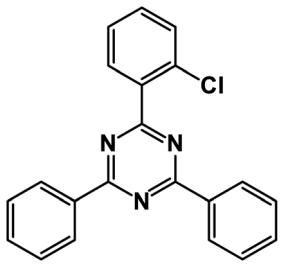

1H NMR (400.1 MHz, CDCl3): $\delta = 8.71$ (d, $J = 3.7$ Hz, 1H), 8.51 (d, $J = 7.9$ Hz, 1H), 8.22 (d, $J = 7.2$ Hz, 2H), 7.92 (s, 1H), 7.88 (s, 1H), 7.73 (d, $J = 6.9$ Hz, 2H), 7.55–7.41 (m, 6H). 13C{1H} NMR (100.6 MHz, CDCl3): $\delta = 159.0$, 156.0, 151.6, 150.1, 147.6, 139.2, 137.7, 135.1, 134.6, 129.4, 129.3, 127.9, 126.2, 126.2, 123.6, 116.8, 116.1.

*2-(4-Bromophenyl)-4,6-di-p-tolyl-1,3,5-triazine (product **3t**).*

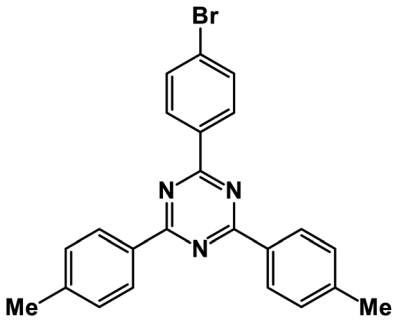

1H NMR (400.1 MHz, CDCl3): $\delta = 8.22$ (d, $J = 7.4$ Hz, 2H), 7.88 (s, 1H), 7.55–7.50 (m, 4H), 7.46–7.43 (m, 3H), 7.33 (d, $J = 7.6$ Hz, 1H), 7.27–7.25 (m, 1H), 13C{1H} NMR (100.6 MHz, CDCl3): $\delta =$ 161.3, 158.6, 151.1, 141.6, 139.7, 131.3, 129.1, 127.8, 126.2, 118.7, 116.2, 113.3, 112.1, 25.5.

Conflicts of interest

There are no conflicts to declare.

Acknowledgements

Tianjin Municipal Education Commission (2020KJ061). Tianjin Training Program of Innovation and Entrepreneurship for Undergraduates (202114038011).

References

1 D. Dharmendra, P. Chundawat, Y. Vyas and C. Ameta, *J. Chem. Sci.*, 2022, **134**, 47.
2 M. Gholinejad, B. Karimi and F. Mansouri, *J. Mol. Catal. Chem.*, 2014, **386**, 20–27.
3 B. Zeynizadeh, E. Gholamiyan and M. Gilanizadeh, *Curr. Chem. Lett.*, 2018, **7**, 121–130.
4 J. Kurian, B. B. Lahiri, M. J. Mathew and J. Philip, *J. Magn. Magn. Mater.*, 2021, **538**, 168233.
5 M. A. Rezvani and A. Imani, *J. Environ. Chem. Eng.*, 2021, **9**, 105009.
6 T. Cheng, D. Zhang, H. Li and G. Liu, *Green Chem.*, 2014, **16**, 3401–3427.
7 T. M. Dhameliya, H. A. Donga, P. V Vaghela, B. G. Panchal, D. K. Sureja, K. B. Bodiwala and M. T. Chhabria, *RSC Adv.*, 2020, **10**, 32740–32820.
8 G. Pal, S. Paul and A. R. Das, *New J. Chem.*, 2014, **38**, 2787–2791.
9 V. K. Booramurthy, R. Kasimani, S. Pandian and D. Subramanian, *Arab. J. Sci. Eng.*, 2022, **47**, 6341–6353.
10 H. Khashei Siuki, P. Ghamari Kargar and G. Bagherzade, *Sci. Rep.*, 2022, **12**, 3771.
11 D. D. Stueber, J. Villanova, I. Aponte, Z. Xiao and V. L. Colvin, *Pharmaceutics*, 2021, **13**, 943.
12 L. Shiri, A. Ghorbani-Choghamarani and M. Kazemi, *Aust. J. Chem.*, 2016, **69**, 585.
13 M. Kazemi and M. Ghobadi, *Nanotechnol. Rev.*, 2017, **6**, 549–571.
14 M. Ghobadi, M. Kargar Razi, R. Javahershenas and M. Kazemi, *Synth. Commun.*, 2021, **51**, 647–669.
15 H. R. Sonawane, J. V. Deore and P. N. Chavan, *ChemistrySelect*, DOI: **10.1002/slct.202103900**.
16 H. Long Ngo, D. Kumar Mishra, V. Mishra and C. Chien Truong, *Chem. Eng. Sci.*, 2021, **229**, 116142.
17 M. Maji, D. Panja, I. Borthakur and S. Kundu, *Org. Chem. Front.*, 2021, **8**, 2673–2709.
18 D. R. Mishra, B. S. Panda, S. Nayak, J. Panda and S. Mohapatra, *ChemistrySelect*, 2022, **7**, e202200531, DOI: **10.1002/slct.202200531**.
19 M. Bashiri, A. Jarrahpour, B. Rastegari, A. Iraji, C. Irajie, Z. Amirghofran, S. Malek-Hosseini, M. Motamedifar, M. Haddadi, K. Zomorodian, Z. Zareshahrabadi and E. Turos, *Monatsh. Chem.*, 2020, **151**, 821–835.
20 S. Singh, M. K. Mandal, A. Masih, A. Saha, S. K. Ghosh, H. R. Bhat and U. P. Singh, *Arch. Pharm.*, 2021, **354**, 2000363.
21 M. KARIMI and A. R. KARIMI, *J. Chil. Chem. Soc.*, 2014, **59**, 2674–2676.
22 A. I. Khodair, A. A. El-Barbary, D. R. Imam, N. A. Kheder, F. Elmalki and T. Ben Hadda, *Carbohydr. Res.*, 2021, **500**, 108246.
23 E. Havránková, J. Csöllei and P. Pazdera, *Molecules*, 2019, **24**, 3586.
24 C. Zhang, M.-T. Ban, K. Zhu, L.-Y. Zhang, Z.-Y. Luo, S.-N. Guo, D.-M. Cui and Y. Zhang, *Org. Lett.*, 2017, **19**, 3947–3949.
25 F. Wang, Z. Deng, Y. Wang, F. Yuan, X. Zhang, G.-P. Lu, N. Fu and Y. Lin, *Tetrahedron*, 2022, **123**, 132985.
26 Q. You, F. Wang, C. Wu, T. Shi, D. Min, H. Chen and W. Zhang, *Org. Biomol. Chem.*, 2015, **13**, 6723–6727.
27 A. R. Tiwari, T. Akash and B. M. Bhanage, *Org. Biomol. Chem.*, 2015, **13**, 10973–10976.
28 F. Xie, M. Chen, X. Wang, H. Jiang and M. Zhang, *Org. Biomol. Chem.*, 2014, **12**, 2761–2768.
29 X. Zhang, H. Liu, X. Sheng, X. Mai, S. Hou, B. Li, X. Chen, Y. Li and F. Xie, *J. Catal.*, 2022, **408**, 227–235.
30 G. Shi, F. He, Y. Che, C. Ni and Y. Li, *Russ. J. Gen. Chem.*, 2016, **86**, 380–386.